
On Recoverability of Graph Neural Network Representations

Maxim Fishman^{*1,2} Chaim Baskin^{*2} Evgenii Zheltonozhskii^{*2} Ron Banner¹ Avi Mendelson²

Abstract

Despite their growing popularity, graph neural networks (GNNs) still have multiple unsolved problems, including finding more expressive aggregation methods, propagation of information to distant nodes, and training on large-scale graphs. Understanding and solving such problems require developing analytic tools and techniques. In this work, we propose the notion of *recoverability*, which is tightly related to information aggregation in GNNs, and based on this concept, develop the method for GNN embedding analysis. We define recoverability theoretically and propose a method for its efficient empirical estimation. We demonstrate, through extensive experimental results on various datasets and different GNN architectures, that estimated recoverability correlates with aggregation method expressivity and graph sparsification quality. Therefore, we believe that the proposed method could provide an essential tool for understanding the roots of the aforementioned problems, and potentially lead to a GNN design that overcomes them. The code to reproduce our experiments is available at <https://github.com/Anonymous1252022/Recoverability>.

1. Introduction

Over the last decade, deep learning allowed researchers to tackle multiple hard tasks, previously considered intractable. For example, convolutional neural networks (CNNs) have been successfully applied to computer vision problems such as image classification (He et al., 2016), object detection (Ren et al., 2015), and semantic segmentation (Ronneberger et al., 2015). Nevertheless, while CNNs are successful in processing pixels, multiple other modalities such as 3D

meshes (Wu et al., 2019), social networks (Ribeiro et al., 2017), brain connections (Shapson-Coe et al., 2021), relational databases (Cvitkovic, 2020), citation graphs (Sen et al., 2008), sensor networks (Bloemheuvel et al., 2021) and many others, require the processing of irregular data. As a result, in recent years, researchers have been looking into ways to exploit deep learning methods, such as CNNs, in order to work with graph structured data. Deep learning on graphs and, in particular, graph neural networks (GNNs, Gori et al., 2005; Scarselli et al., 2008; Kipf & Welling, 2017), based on message passing (Gilmer et al., 2017), i.e., iterative updating of a graph node representation based on information aggregated from its neighbors, has become a very popular tool for machine learning with graphs.

Despite their exceptional ability to learn graph-based data representations, GNNs still suffer from some important problems. One issue is related to aggregation method expressiveness. Kipf & Welling (2017) proposed graph convolution networks (GCNs), which aggregate information from neighboring nodes but cannot distinguish between them. To solve this problem, Hu et al. (2020) integrated a self-attention mechanism (Vaswani et al., 2017) into aggregation, proposing graph attention networks (GAT). Another problem is lack of ability to propagate information between distant nodes in the graph. Li et al. (2018) conjectured that this phenomenon is a result of *over-smoothing*, a situation in which node representations become indistinguishable when the number of layers increases. Alon & Yahav (2021) offered another explanation – *over-squashing* of an exponentially growing amount of information into fixed-size vectors. Finally, training on large-scale graphs is a significant obstacle in integrating GNNs in real-life problems. In real-life graphs, the diameter (maximal distance between two nodes) is often small (3–5) even for large graphs. Thus, GCNs with only 3–5 layers must aggregate information from the whole graph to calculate embedding of a single node, which requires a large amount of memory and compute, and also causes a *bottleneck* (Alon & Yahav, 2021). One way to reduce the amount of computation is to use sampling techniques such as SAGE (Hamilton et al., 2017), SAINT (Zeng et al., 2020), or clustering (Chiang et al., 2019). Another way is to sparsify the graph by dropping a subset of edges (Srinivasa et al., 2020; Rathee et al., 2021).

In this work, we introduce the notion of *recoverability* and

^{*}Equal contribution ¹Habana Labs – An Intel company, Caesarea, Israel ²Technion – Israel Institute of Technology, Haifa, Israel. Correspondence to: Chaim Baskin <chaimbaskin@campus.technion.ac.il>.

demonstrates its tight relationship to information aggregation in GNNs. Recoverability provides an alternative insight into the aforementioned problems and can serve as a good tool for understanding their roots and finding solutions for them. First, we provide a qualitative definition of recoverability and its empirical counterpart, recoverability loss. We then use reproducing kernel Hilbert space (RKHS) embedding for estimating recoverability loss in an efficient and differentiable way. Finally, we show how to use recoverability for measuring the quality of embedding method. The main idea behind recoverability is visualized in Fig. 1, where we can see how recoverability loss ρ changes when the input graph is sparsified. When the graph is sparser the recoverability loss is higher. We can use this effect to understand why some sparsification methods are better than others, and potentially propose better ones in the future.

Our contributions in this work are:

- We show that recoverability and recoverability loss are closely related to information aggregation in GNNs.
- By embedding into RKHSs, we demonstrate an efficient and differentiable method of estimating the recoverability loss.
- Based on the notion of recoverability, we develop a method for GNN embedding analysis.
- We provide extensive experimental results on various datasets and GNN architectures demonstrate that estimated recoverability correlates with the expressiveness of the selected aggregation method and graph sparsification quality.

2. Related work

Embedding methods are important for using graphs in deep learning. Thus, it is essential to develop theoretical tools to analyze their representational properties and limitations. Xu et al. (2019) proposed a theoretical framework for analyzing the expressive power of GNNs to capture different graph structures. They also developed a simple architecture that is the most expressive among the class of GNNs and is as powerful as the Weisfeiler-Leman graph isomorphism test (Leman & Weisfeiler, 1968). Li et al. (2018) showed that the GCN model is a particular form of Laplacian smoothing and raised the concern of *oversmoothing* with many convolutional layers, which prevents the propagation of information to distant nodes. Alon & Yahav (2021) proposed an alternative explanation to the problem of information propagation: GNNs are susceptible to a *bottleneck* when aggregating messages across a long path. This bottleneck causes the *over-squashing* of exponentially growing information into fixed-size vectors. Topping et al. (2021) introduced a new

edge-based combinatorial curvature and proved that negatively curved edges are responsible for the over-squashing issue.

In our work, we demonstrate an alternative approach to embedding method analysis based on the amount of information aggregated in the embedding. A few works that utilized information-theoretic tools in GNNs already exist. (Peng et al., 2020; Bandyopadhyay et al., 2020; Sun et al., 2020) use a mutual information (MI) maximization technique for learning better graph representations. In those works, MI is estimated via MINE (Belghazi et al., 2018) or its improvement, MI-NEE (Chan et al., 2019), which involves a lot of additional parameters that should be learned for correct MI estimation. We eliminate MI estimation in our work by turning to functional analytic tools. We define recoverability and use RKHS (Aronszajn, 1950) embedding, a popular approach in machine learning toolbox (Hofmann et al., 2008; Muandet et al., 2017; Klebanov et al., 2021), with a universal kernel (Micchelli et al., 2006) for its estimation. In the context of bias-variance decomposition (Geman et al., 1992; Domingos, 2000; Yang et al., 2020), recoverability measures the amount of noise in the loss.

3. Method

We characterize neural graph embedding as having three parameters: an aggregation algorithm, a certain number of layers, and a graph sparsification algorithm. Our goal is to compare different embeddings based on those parameters and see which one performs better on the given data. To achieve this goal, we define a method for analyzing neural graph embeddings. First, the problem of measuring the quality of a given embedding is reduced to the problem of determining how well one can recover one random variable from another. Second, we define a new concept of recoverability and recoverability loss. Third, we demonstrate how to compute recoverability loss in a differentiable and efficient way. Finally, we present an algorithm for measuring graph embedding quality using recoverability.

3.1. From an embedding to recoverability

In the node property prediction task, given graph $G = (V, E)$ equipped with node features $\mathcal{X} = \{x_v\}_{v \in V}$ and labels $\mathcal{Y} = \{y_v\}_{v \in V}$ distributed according to some probability distribution $(x_v, y_v) \sim (X, Y)$, one should predict the label of each node in the graph. To solve this task we embed the graph with node features (G, \mathcal{X}) into a latent space, acquiring some representation of each node, which we denote as $h_v \sim H$, and then apply a classifier to the embedding h_v , trying to predict label y_v .

The success of the above procedure is highly dependent on the ability to learn a map between random variables H and

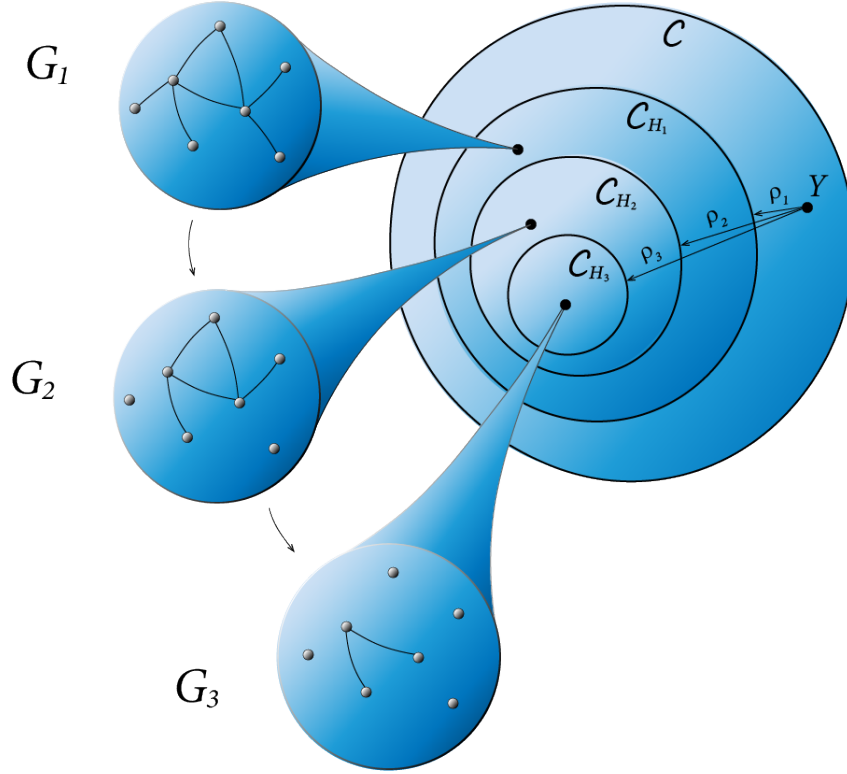


Figure 1. The relation between graph sparsification and recoverability loss. G_2 and G_3 are sparsified versions of graph G_1 , and Y is the node class random variable. The fewer edges the graph G_i has, the smaller the correspondent space \mathcal{C}_{H_i} is, and, consequently, recoverability loss ρ is higher.

Y . Since different embedding methods produce different random variables, we can reduce the problem of measuring the embedding method’s quality to measuring the ability to learn random variable Y from random variable H . This leads to the natural question of how much information do we have in random variable H to recover Y . We term the ability to recover Y from a given H *recoverability*. One way to estimate recoverability is by using information theoretic tools, but these require an intermediate density estimation that could be intractable in higher dimensions. Another way, which is less arduous and more appealing, is to use functional analysis tools. We demonstrate the latter option below in Sections 3.2 to 3.4

3.2. Recoverability and recoverability loss

Given two random variables H and Y , with the values in $U \subset \mathbb{R}^d$ and \mathbb{R} , respectively, we say that Y is fully recoverable from H if there exists a continuous function $f : U \rightarrow \mathbb{R}$ such that $f(H) = Y$. In the general case, however, we do not have such a relation between H and Y , which means that we cannot fully recover Y from H . Nevertheless, H may still contain some information from which we can partially recover Y . To measure the amount of such information in

H , we define the following set:

$$\mathcal{C}_H = \{f(H) \mid f : U \rightarrow \mathbb{R} \text{ is continuous function}\} \quad (1)$$

i.e., the collection of all random variables that could be fully recovered from H , and then evaluate the distance between random variable Y and the set \mathcal{C}_H :

$$\rho(Y|H) = \inf_{Z \in \mathcal{C}_H} d(Y, Z) \quad (2)$$

where d is some distance function. We denote the value $\rho(Y|H)$ as the recoverability loss. If $\rho(Y|H) = 0$, then there exists a continuous function f such that $f(H) = Y$ and thus Y is fully recoverable from H . If we are given two different random variables H_1 and H_2 (i.e., two different embeddings of (G, X)) such that $\rho(Y|H_1) < \rho(Y|H_2)$, then Y is more recoverable from H_1 than from H_2 (which means that embedding method 1 is better than method 2). The last case is demonstrated in Fig. 2.

If we extend the collection of continuous functions in \mathcal{C}_H to the measurable functions, and take as distance d the one induced from the L_2 norm on random variables, then the $Z \in \mathcal{C}_H$ that minimizes $\rho(Y|H)$ is almost everywhere equivalent to conditional expectation $\mathbb{E}[Y|H]$. Consequently, conditional expectation $\mathbb{E}[Y|H]$ can be used for testing $\rho(Y|H)$ values on synthetic data.

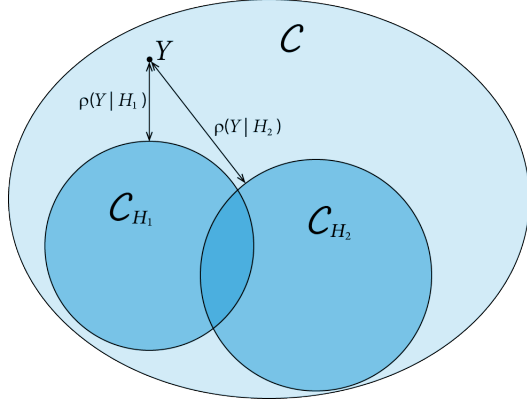


Figure 2. For random variables H_i , C_{H_i} is the collection of all random variables that are fully recoverable from H_i . The distance from random variable Y $\rho(Y|H_1)$ is smaller than $\rho(Y|H_2)$, and thus Y is better recoverable from H_1 than from H_2 .

The traditional bias-variance decomposition decomposes the loss for a given loss function L on a dataset $D = \{(x_i, y_i)\}$ as a sum of three factors (Domingos, 2000):

$$\mathcal{L}(x) = \underbrace{\mathbb{E}_D[L(\hat{y}, y_m)]}_{\text{Var}} + \underbrace{L(y_m, y_*)}_{\text{Bias}^2} + \underbrace{\mathbb{E}_y[L(y_*, y)]}_{\text{noise}}. \quad (3)$$

Here \hat{y} is our prediction, y_* is an optimal prediction (i.e., one that minimizes $\mathbb{E}_y[L(y_*, y)]$ for a given sample), and y_m is the main prediction (i.e., one that minimizes $\mathbb{E}_D[L(\hat{y}, y_m)]$ for a given dataset). Differently from many previous works, we focus on quantifying the “noise” term of this decomposition. In other words, we want to know how well we can predict the target in the optimal case.

3.3. Recoverability loss estimation with RKHS

Let $U \subset \mathbb{R}^d$ be compact,¹

$$C(U) = \{f : U \rightarrow \mathbb{R} \mid f \text{ continuous}\}, \quad (4)$$

and \mathcal{H} be an RKHS built from the following kernel:

$$\forall h_1, h_2 \in U \quad k(h_1, h_2) = \exp\left(-\frac{\|h_1 - h_2\|^2}{2\sigma^2}\right). \quad (5)$$

By virtue of the universality property (Micchelli et al., 2006) of the chosen kernel, we can consider only the functions in \mathcal{H} instead of those in the whole $C(U)$.

Lemma 1 *The recoverability loss is given by*

$$\rho(Y|H) = \inf_{f \in \mathcal{H}} d(Y, \langle f, \phi_h(\cdot) \rangle), \quad (6)$$

¹It is not a restrictive assumption that U is compact since all tensor values in neural networks are bounded.

where

$$\forall h \in U \quad \phi_h(\cdot) = k(h, \cdot) \quad (7)$$

and $\langle \cdot, \cdot \rangle$ is inner product in \mathcal{H} .

We denote the estimation of ρ on a finite collection of samples $(\mathcal{H}, \mathcal{Y}) = \{(h_n, y_n)\}_{n \in [N]}$ by ρ^* and use the distance induced from the L_p -norm, where $p \in [1, \infty)$.

Now we can apply the *representer theorem* (Kimeldorf & Wahba, 1970) to Lemma 1:

Lemma 2 *Recoverability loss is approximated as*

$$\rho^*(Y|H) = \min_{\alpha \in \mathbb{R}^N} \frac{1}{N^{1/p}} \|y - K\alpha\|_p \quad (8)$$

where $K_{ij} = k(h_i, h_j)$ is a Gram matrix.

Finally, we can get rid of parameters $\alpha \in \mathbb{R}^n$.

Theorem 1 *Recoverability loss is given by*

$$\rho^*(Y|H) = \frac{1}{N^{1/p}} \|(\mathbb{I} - \Pi)y\|_p, \quad (9)$$

where Π is an orthogonal projection to the $\text{Im}(K)$ and \mathbb{I} is an identity matrix, and thus Algorithm 1 provides estimation of recoverability loss.

We provide proofs of all these statements in Appendix A.

3.4. Embedding quality estimation

An algorithm. We now provide an algorithm that measures the quality of a given embedding method. Suppose we are given a graph $G = (V, E)$ with node features $x_n \sim X$, node classes $y_n \sim Y$ and two different embedding methods EM_1 and EM_2 , which produce two representations $h_n^1 \sim H_1$ and $h_n^2 \sim H_2$, respectively. If $\rho(Y|H_1) < \rho(Y|H_2)$, then Y is more recoverable from H_1 than from H_2 . In this case, embedding method EM_1 is better than EM_2 . We use this for measuring the quality of given embedding method EM , as summarized in Algorithm 2. First, we apply embedding method EM to $(G, \{x_n\}_{n \in [N]})$ to produce $h_n \sim H$, which is equivalent in time to a single forward pass of GNN on the full graph. We then use $\{h_n\}_{n \in N}$ to estimate $\rho(Y|H)$ using Algorithm 1. The time complexity of Algorithm 1 is $\mathcal{O}(Nm^2)$, where N is the number of nodes in the graph and m is the batch size of Algorithm 1. This allows fast approximation of the recoverability loss, as compared to training a GNN model on a given dataset.

Aggregation method quality. To evaluate the quality of the aggregation part of some embedding method, we fix learnable parameters as identities and apply the resulting

Algorithm 1 $\rho(Y|H)$ estimation.

Input: $\{(h_n, y_n)\}_{n \in [N]}$
Output: $\rho^*(Y|H)$
for j^{th} batch $\{(\tilde{h}_i, \tilde{y}_i)\}_{i \in [m]} \subseteq \{(h_n, y_n)\}_{n \in [N]}$ **do**
 Compute distance matrix
 $K_{kl} \leftarrow \exp\left(-\frac{\|\tilde{h}_k - \tilde{h}_l\|^2}{2\sigma^2}\right)$
 Compute eigendecomposition $K = U^{-1}\Lambda U$ of K
 $U, \Lambda \leftarrow \text{eig}(K)$
 Compute projection to $\text{im}(K)$
 $\Pi \leftarrow \sum_{\lambda_i > 0} u_i u_i^T$
 $\rho_j^*(Y|H) \leftarrow \frac{1}{m^{1/p}} \|(\Pi - \Pi)\tilde{y}\|_p$
end for
 $\rho^*(Y|H) = \frac{m}{N} \sum_j \rho_j^*(Y|H)$

Algorithm 2 Embedding method quality.

Input: $(G, \{x_n\}_{n \in [N]})$, $\{y_n\}_{n \in [N]}$ and embedding method EM
Output: embedding method EM quality
 Generate outcomes of H
 $\{h_n\}_{n \in [N]} \leftarrow \text{EM}((G, \{x_n\}_{n \in [N]}))$
 Use Algorithm 1 to estimate ρ
 $\rho^*(Y|H) \leftarrow \text{Algorithm 1}(\{(h_n, y_n)\}_{n \in [N]})$

layer to the graph multiple times, defining an embedding method EM, which can be evaluated using Algorithm 2. For example, for SAGEConv (Hamilton et al., 2017), defined as follows:

$$x'_i = W_1 \cdot x_i + W_2 \cdot \text{mean}_{j \in N(i)} \{x_j\}, \quad (10)$$

we fix matrices W_1 and W_2 to identity.

Sparsification method quality. Similarly, to evaluate sparsification, we apply sparsification SM to the graph G , producing a sparser graph $\tilde{G} = (V, \tilde{E})$. Then we use Algorithm 2 with $(\tilde{G}, \{x_n\}_{n \in [N]})$, $\{y_n\}_{n \in [N]}$ and embedding method EM as input, as shown in Fig. 1.

4. Experiments

In this section, we show the effectiveness of the recoverability metric on synthetic data and provide extensive experimental results on real datasets and different GNN architectures, where we show various applications of the proposed method for graph embedding analysis.

4.1. Synthetic data

We start with experiments on synthetic data, in which the value of ρ can be calculated analytically, to demonstrate

	ρ^* (mean \pm std)	ρ
$\rho^*(X Z)$	0.119 \pm 0.004	0
$\rho^*(X W)$	0.974 \pm 0.026	1
$\rho^*(Z X)$	0.099 \pm 0.013	0
$\rho^*(W X)$	0.110 \pm 0.019	0

Table 1. The estimated distance from X to \mathcal{C}_W is larger than the distance from X to \mathcal{C}_Z , since we cannot fully recover X from W .

the performance of our estimation approach, at least in the simple case. To demonstrate the ability of recoverability to capture the existence of a continuous map from one random variable to another, we use a simple 1D experiment. Let X be a normally distributed random variable, and let Z and W be defined as follows:

$$Z = f_1(X) = \text{sign}(X) \cdot X^2 \quad (11)$$

$$W = f_2(X) = X^2. \quad (12)$$

Since f_1 is invertible and f_2 is not, we can fully recover X from Z but not from W . Of course, we can fully recover Z and W from X , since we explicitly defined continuous maps f_1 and f_2 .

For this test we generated 1000 samples of X and estimated ρ^* with Algorithm 1. The results are shown in Table 1.

Now, let X and N be 100-dimensional random vectors, with independent normally distributed entries, and Y be defined as

$$Y = \sum_{i \in [100]} (X_i + \alpha \cdot N_i), \quad (13)$$

where α is some parameter. When α tends to zero, Y can be fully recovered from X , and when $|\alpha|$ is large, the noise N dominates the value of X , and consequently Y cannot be recovered from X . This behavior is visualized in Fig. 3, where $\rho^*(Y|X)$, estimated on 1000 samples, is compared to its theoretical value (the calculation is given in Appendix B).

4.2. Real-world data

We now turn to real-world data, and show that the quality of embedding, measured by classification accuracy in the node classification task, is strongly correlated with recoverability.

4.2.1. EXPERIMENTAL SETTING

Dataset statistics, used in the following experiments, are summarized in Table 2.

Throughout the experiments we use five different embedding layers²: GCNConv (Kipf & Welling, 2017), SAGEConv (Hamilton et al., 2017), GINConv (Xu et al., 2019),

²The notation is taken from PyTorch Geometric (Fey &

On Recoverability of Graph Neural Network Representations

Name	Nodes	Edges	Feature dim.	Classes	Multilabel	Train	Val	Test	Directed	Homophily
Reddit2	232,965	11,606,919	602	41	–	153,932	23,699	55,334	–	0.782
ogbn-arxiv	169,343	1,166,243	128	40	–	90,941	29,799	48,603	✓	0.654
Flickr	89,250	449,878	500	7	–	44,625	22,312	22,313	–	0.319
PPI	56,944	793,632	50	121	✓	44,906	6,514	5,524	–	0.620 [†]
ogbn-products	2,449,029	61,859,140	100	47	–	196,615	39,323	2,213,091	–	0.808

Table 2. Dataset statistics. [†] The homophily of PPI is the average over all classes.

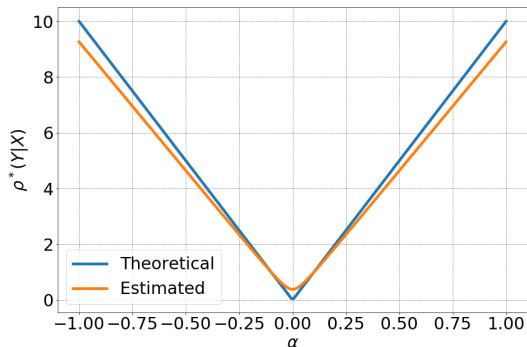


Figure 3. Comparison between estimated $\rho^*(Y|X)$ and its theoretical value for different α .

GraphConv (Morris et al., 2019), and GATv2Conv (Brody et al., 2022). More details on the embedding layers are given in Appendix C.

For experimental purposes, we separate the embedding part from the classifier part in a GNN model, as described in Section 3.1. Therefore, for training, we use a GNN model consisting of two consecutive blocks, where the first block is an embedding built from $k \in \{1 \dots 9\}$ layers of one of the considered types, and the second block is a classifier consisting of three fully connected layers. Each layer except for the last one is followed by ReLU activation and dropout.

4.2.2. EXPERIMENTS

The usefulness of edges. The first experiment shows an interesting property of the datasets appearing in Table 2, which could help elucidate why GNNs with a SAGEConv layer can be used efficiently for training on these. We took three consecutive SAGEConv layers without learnable parameters as embedding method EM, i.e., only the aggregation parts (as shown in Section 3.4), and applied it to the node features. Let X denote the random variable of node features, H the node embedding (after EM application) and Y the node classes. From Table 3 we can see that $\rho^*(Y|H) < \rho^*(Y|X)$. In other words, Y is more recoverable from H (node embedding) than from X (node features).

(Lensen, 2019).

Dataset	$\rho^*(Y X)$	$\rho^*(Y H)$
Reddit2	0.088	0.066
ogbn-arxiv	0.085	0.079
Flickr	0.188	0.183
PPI	0.374	0.287
ogbn-products	0.041	0.017

Table 3. The recoverability loss ρ before and after application of embedding method EM. One can see how recoverability loss ρ decreases when embedding method EM is applied to the node features.

Additionally, we observe an interesting correlation between recoverability loss drop and homophily. In the Reddit2 and ogbn-products datasets, which have a relatively high homophily, the recoverability loss drops relatively sharply, whereas in the Flickr dataset, which has a relatively low homophily, the recoverability loss changes relatively slightly.

Correlation between recoverability and aggregation method quality. This experiment shows the correlation between recoverability loss and aggregation method quality on a given dataset, i.e., the test accuracy after the training on a GNN model defined in Section 4.2.1. The results are shown in Figs. 4 to 8, where the y axis is the test accuracy of the trained GNN model on a given dataset, and the x axis is the inverse of the estimated recoverability loss. For GraphConv, GCNConv, SAGEConv and GINConv, the estimation of recoverability loss was done only on the aggregation part, according to Section 3.4. For GATv2Conv, the recoverability loss was computed for the node embedding of the trained model. From all plots it can be seen that as the recoverability loss drops, the test accuracy becomes higher.

Propagation of information to distant nodes. This experiment demonstrates the depth problem in GNNs and its correlation with the recoverability. We took two GNN models with three and nine embedding layers of type SAGEConv each (the model is defined in Section 4.2.1), and trained them on datasets from Table 2. The results are given in Table 4. For the Reddit2, ogbn-arxiv and ogbn-products datasets, we did not see a significant change in test accuracy after the training, whereas for the Flickr and PPI

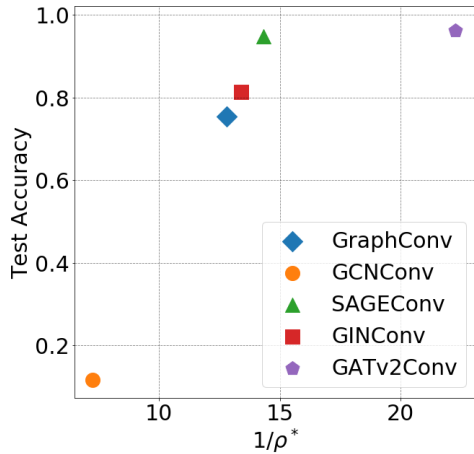


Figure 4. The correlation between the test accuracy and the recoverability loss for Reddit2 dataset.

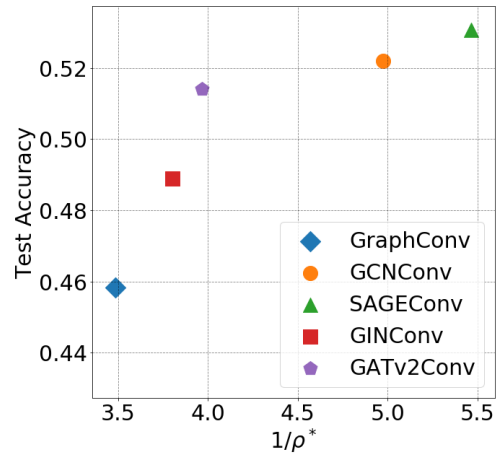


Figure 6. The correlation between the test accuracy and the recoverability loss for Flickr dataset.

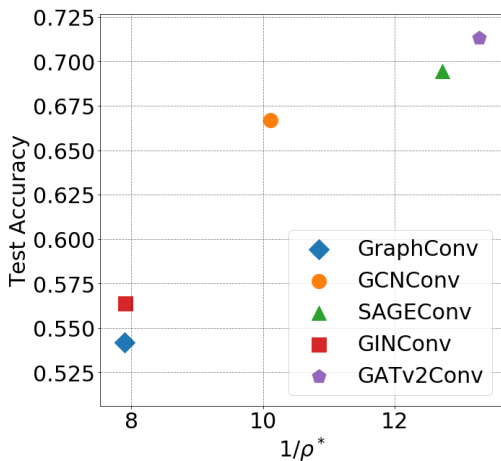


Figure 5. The correlation between the test accuracy and the recoverability loss for ogbn-arxiv dataset.

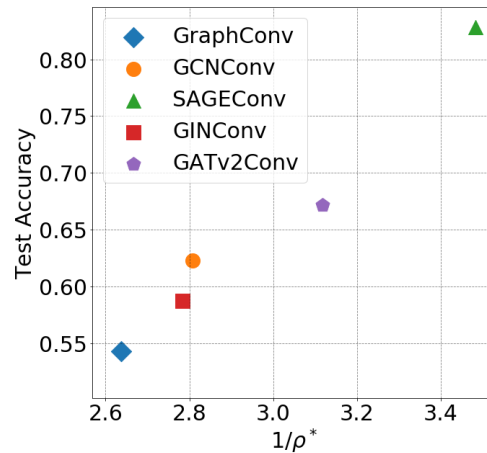


Figure 7. The correlation between the test accuracy and the recoverability loss for PPI dataset.

datasets, there was a degradation in accuracy for nine-layer architecture. We collected the recoverability loss of each embedding layer in the trained nine-layer architecture. The results are shown in Fig. 9. For Reddit2, ogbn-arxiv and ogbn-products, we have a similar pattern of ρ behavior: it smoothly decreases, meaning that each consecutive layer aggregates more and more information to recover Y . For Flickr and PPI, we see different behavior. In Flickr, ρ increases, indicating that it does not aggregate any useful information from neighboring nodes to recover Y . In PPI, ρ first decreases and starts to increase after three layers, which indicates that the *over-smoothing* or *over-squashing* problem is occurring.

Correlation between recoverability and the graph sparsification method quality. In this experiment we show that the quality of the given sparsification method correlates

Dataset	Accuracy	
	3 layers	9 layers
Reddit2	0.946	0.943
ogbn-arxiv	0.692	0.691
ogbn-products	0.789	0.792
Flickr	0.532	0.522
PPI	0.831	0.761

Table 4. Test accuracy of trained models with three and nine SAGEConv embedding layers.

with recoverability. We use two simple sparsification methods. In **Random** sparsification we randomly drop 90% of the edges from the graph. In **Max d** sparsification we find

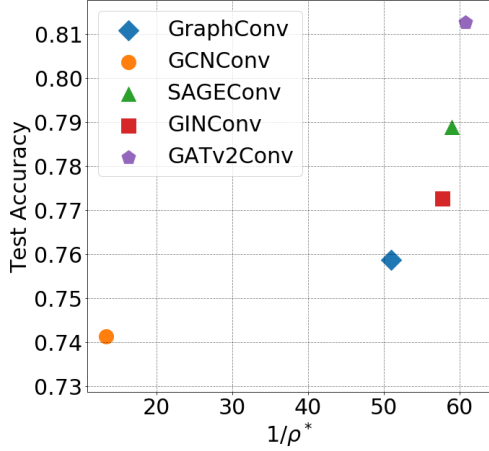


Figure 8. The correlation between the test accuracy and the recoverability loss for ogbn-products dataset.

Dataset	Sparsification	
	Random	Max d
Reddit2	0.083 / 0.906	0.069 / 0.938
ogbn-arxiv	0.109 / 0.568	0.084 / 0.586
Flickr	0.214 / 0.466	0.191 / 0.470
PPI	0.313 / 0.598	0.266 / 0.617
ogbn-products	0.020 / 0.705	0.017 / 0.767

Table 5. Comparison of two sparsification methods, where 90% of the edges were dropped from the graphs. Each element in the table is “ ρ / test accuracy”. One can see the correlation between recoverability loss and the test accuracy.

the maximal value of d that satisfies

$$\sum_{v \in V} \min\{d, d_{\text{in}}(v)\} \leq 0.1|E|, \quad (14)$$

where $d_{\text{in}}(v)$ is an input degree of v , and for each node v in the graph we randomly leave $\min\{d, d_{\text{in}}(v)\}$ of input edges. Both methods leave 10% of the edges in the graph.

To evaluate quality of sparsification, we first apply it to the given dataset and then train a three-layer SAGEConv GNN mode (defined in Section 4.2.1) on sparsified data. We also compute the recoverability loss of the aggregation part, as described in Section 3.4. The results are shown in Table 5. We see that the **Max d** sparsification is better than **Random**, and correspondingly, the recoverability loss of **Max d** is lower than that of **Random**.

5. Conclusions

In this work, we defined recoverability, provided an efficient and differentiable method for estimation of recoverability loss and showed how it can be used for measuring the quality

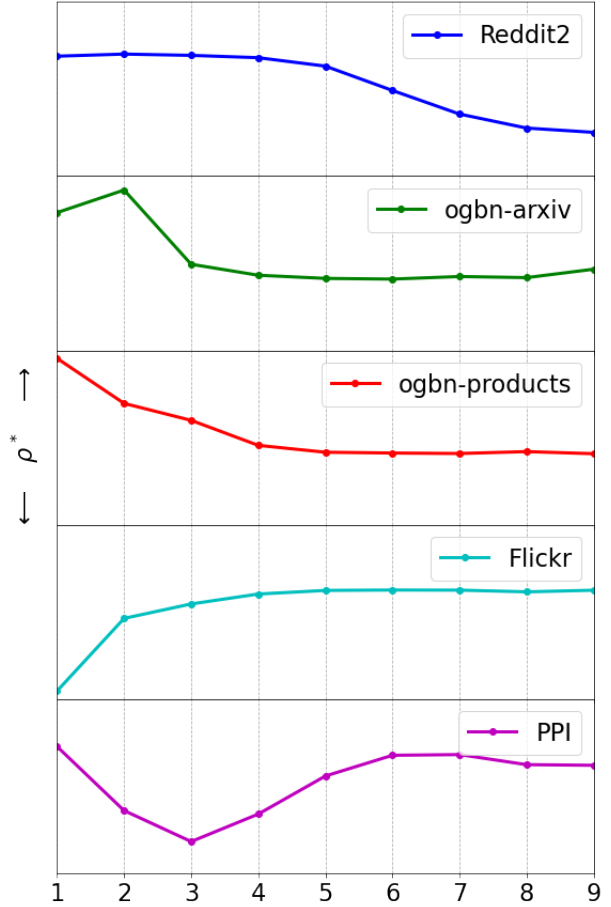


Figure 9. The recoverability loss of each embedding layer in trained GNN model. The recoverability of the Flickr and PPI datasets behaves differently than the recoverability of the Reddit2, ogbn-arxiv and ogbn-products datasets.

of GNN embedding. We demonstrated empirically that recoverability is tightly related to information aggregation in GNNs across various datasets and multiple architectures. We show that the behavior of recoverability correlates with aggregation and sparsification method quality and how it can be used for depth problem analysis. Computing the recoverability loss is efficient and does not require training, and thus can be done quickly on large datasets. To conclude, the notion of recoverability could provide an essential tool for understanding the roots of and providing better solutions for the problems with GNNs, such as the expressiveness of the aggregation method, propagation of information to distant nodes and training on large-scale graphs.

Acknowledgements

This research was supported by the Technion Hiroshi Fujiwara Cyber Security Research Center and the Israel National Cyber Directorate.

References

- Alon, U. and Yahav, E. On the bottleneck of graph neural networks and its practical implications. In *International Conference on Learning Representations*, 2021. URL <https://openreview.net/forum?id=i800PhOCVH2>. (cited on pp. 1 and 2)
- Aronszajn, N. Theory of reproducing kernels. *Transactions of the American mathematical society*, 68(3):337–404, 1950. (cited on p. 2)
- Bandyopadhyay, S., Aggarwal, M., and Murty, M. N. Un-supervised graph representation by periphery and hierarchical information maximization. *arXiv preprint arXiv:2006.04696*, 2020. URL <https://arxiv.org/abs/2006.04696>. (cited on p. 2)
- Belghazi, M. I., Baratin, A., Rajeswar, S., Ozair, S., Bengio, Y., Courville, A., and Hjelm, R. D. MINE: mutual information neural estimation. *arXiv preprint arXiv:1801.04062*, 2018. URL <https://arxiv.org/abs/1801.04062>. (cited on p. 2)
- Bloemheuvel, S., van den Hoogen, J., and Atzmueller, M. A computational framework for modeling complex sensor network data using graph signal processing and graph neural networks in structural health monitoring. *arXiv preprint arXiv:2105.05316*, 2021. (cited on p. 1)
- Brody, S., Alon, U., and Yahav, E. How attentive are graph attention networks? In *International Conference on Learning Representations*, 2022. URL <https://openreview.net/forum?id=F72ximsx7C1>. (cited on p. 6)
- Chan, C., Al-Bashabsheh, A., Huang, H. P., Lim, M., Tam, D. S. H., and Zhao, C. Neural entropic estimation: A faster path to mutual information estimation, 2019. (cited on p. 2)
- Chiang, W.-L., Liu, X., Si, S., Li, Y., Bengio, S., and Hsieh, C.-J. Cluster-gcn. *Proceedings of the 25th ACM SIGKDD International Conference on Knowledge Discovery & Data Mining*, Jul 2019. doi: 10.1145/3292500.3330925. URL <http://dx.doi.org/10.1145/3292500.3330925>. (cited on p. 1)
- Cvitkovic, M. Supervised learning on relational databases with graph neural networks. *arXiv preprint arXiv:2002.02046*, 2020. (cited on p. 1)
- Domingos, P. A unified bias-variance decomposition and its applications. In *Proceedings of the Seventeenth International Conference on Machine Learning, ICML '00*, pp. 231–238, San Francisco, CA, USA, 2000. Morgan Kaufmann Publishers Inc. ISBN 1558607072. (cited on pp. 2 and 4)
- Fey, M. and Lenssen, J. E. Fast graph representation learning with PyTorch geometric, May 2019. URL https://github.com/pyg-team/pytorch_geometric. (cited on p. 5)
- Geman, S., Bienenstock, E., and Doursat, R. Neural Networks and the Bias/Variance Dilemma. *Neural Computation*, 4(1):1–58, 01 1992. ISSN 0899-7667. doi: 10.1162/neco.1992.4.1.1. URL <https://doi.org/10.1162/neco.1992.4.1.1>. (cited on p. 2)
- Gilmer, J., Schoenholz, S. S., Riley, P. F., Vinyals, O., and Dahl, G. E. Neural message passing for quantum chemistry. In Precup, D. and Teh, Y. W. (eds.), *Proceedings of the 34th International Conference on Machine Learning*, volume 70 of *Proceedings of Machine Learning Research*, pp. 1263–1272. PMLR, 06–11 Aug 2017. URL <https://proceedings.mlr.press/v70/gilmer17a.html>. (cited on p. 1)
- Gori, M., Monfardini, G., and Scarselli, F. A new model for learning in graph domains. In *Proceedings. 2005 IEEE International Joint Conference on Neural Networks, 2005.*, volume 2, pp. 729–734. IEEE, 2005. (cited on p. 1)
- Hamilton, W., Ying, Z., and Leskovec, J. Inductive representation learning on large graphs. In Guyon, I., Luxburg, U. V., Bengio, S., Wallach, H., Fergus, R., Vishwanathan, S., and Garnett, R. (eds.), *Advances in Neural Information Processing Systems*, volume 30. Curran Associates, Inc., 2017. URL <https://proceedings.neurips.cc/paper/2017/hash/5dd9db5e033da9c6fb5ba83c7a7e9bea9-Abstract.html>. (cited on pp. 1 and 5)
- He, K., Zhang, X., Ren, S., and Sun, J. Deep residual learning for image recognition. In *Proceedings of the IEEE Conference on Computer Vision and Pattern Recognition (CVPR)*, June 2016. URL https://www.cv-foundation.org/openaccess/content_cvpr_2016/html/He_Deep_Residual_Learning_CVPR_2016_paper.html. (cited on p. 1)
- Hofmann, T., Schölkopf, B., and Smola, A. J. Kernel methods in machine learning. *The Annals of Statistics*, 36(3), Jun 2008. ISSN 0090-5364. doi: 10.1214/009053607000000677. URL <http://dx.doi.org/10.1214/009053607000000677>. (cited on p. 2)
- Hu, W., Liu, B., Gomes, J., Zitnik, M., Liang, P., Pande, V., and Leskovec, J. Strategies for pre-training graph neural networks. In *International Conference on Learning Representations*, 2020. URL <https://openreview.net/forum?id=HJlWWJSFDH>. (cited on p. 1)

- Kimeldorf, G. S. and Wahba, G. A correspondence between Bayesian estimation on stochastic processes and smoothing by splines. *The Annals of Mathematical Statistics*, 41(2):495 – 502, 1970. doi: 10.1214/aoms/1177697089. URL <https://doi.org/10.1214/aoms/1177697089>. (cited on pp. 4 and 12)
- Kipf, T. N. and Welling, M. Semi-supervised classification with graph convolutional networks. In *International Conference on Learning Representations*, 2017. URL <https://openreview.net/forum?id=SJU4ayYgl>. (cited on pp. 1 and 5)
- Klebanov, I., Sprungk, B., and Sullivan, T. J. The linear conditional expectation in Hilbert space. *Bernoulli*, 27(4):2267 – 2299, 2021. doi: 10.3150/20-BEJ1308. URL <https://doi.org/10.3150/20-BEJ1308>. (cited on p. 2)
- Leman, A. A. and Weisfeiler, B. Y. A reduction of a graph to a canonical form and an algebra arising during this reduction. *Nauchno-Tekhnicheskaya Informatsiya*, 2(9): 12–16, 1968. (cited on p. 2)
- Li, Q., Han, Z., and Wu, X.-M. Deeper insights into graph convolutional networks for semi-supervised learning. *Proceedings of the AAAI Conference on Artificial Intelligence*, 32(1), Apr. 2018. URL <https://ojs.aaai.org/index.php/AAAI/article/view/11604>. (cited on pp. 1 and 2)
- Micchelli, C. A., Xu, Y., and Zhang, H. Universal kernels. *Journal of Machine Learning Research*, 7(95):2651–2667, 2006. URL <http://jmlr.org/papers/v7/micchelli06a.html>. (cited on pp. 2, 4, and 12)
- Morris, C., Ritzert, M., Fey, M., Hamilton, W. L., Lenssen, J. E., Rattan, G., and Grohe, M. Weisfeiler and Leman go neural: Higher-order graph neural networks. *Proceedings of the AAAI Conference on Artificial Intelligence*, 33(01):4602–4609, Jul. 2019. doi: 10.1609/aaai.v33i01.33014602. URL <https://ojs.aaai.org/index.php/AAAI/article/view/4384>. (cited on p. 6)
- Muandet, K., Fukumizu, K., Sriperumbudur, B., and Schölkopf, B. Kernel mean embedding of distributions: A review and beyond. *Foundations and Trends® in Machine Learning*, 10(1-2):1–141, 2017. ISSN 1935-8245. doi: 10.1561/22000000060. URL <http://dx.doi.org/10.1561/22000000060>. (cited on p. 2)
- Peng, Z., Huang, W., Luo, M., Zheng, Q., Rong, Y., Xu, T., and Huang, J. Graph representation learning via graphical mutual information maximization. In *Proceedings of The Web Conference 2020*, pp. 259–270, New York, NY, USA, 2020. Association for Computing Machinery. ISBN 9781450370233. URL <https://doi.org/10.1145/3366423.3380112>. (cited on p. 2)
- Rathee, M., Zhang, Z., Funke, T., Khosla, M., and Anand, A. Learnt sparsification for interpretable graph neural networks. *arXiv preprint arXiv:2106.12920*, 2021. URL <https://arxiv.org/abs/2106.12920>. (cited on p. 1)
- Ren, S., He, K., Girshick, R., and Sun, J. Faster R-CNN: Towards real-time object detection with region proposal networks. In Cortes, C., Lawrence, N., Lee, D., Sugiyama, M., and Garnett, R. (eds.), *Advances in Neural Information Processing Systems*, volume 28. Curran Associates, Inc., 2015. URL <https://proceedings.neurips.cc/paper/2015/hash/14bfa6bb14875e45bba028a21ed38046-Abstract.html>. (cited on p. 1)
- Ribeiro, M. H., Calais, P. H., Santos, Y. A., Almeida, V. A. F., and Meira Jr, W. “Like sheep among wolves”: Characterizing hateful users on twitter. *arXiv preprint arXiv:1801.00317*, 2017. (cited on p. 1)
- Ronneberger, O., Fischer, P., and Brox, T. U-net: Convolutional networks for biomedical image segmentation. In *International Conference on Medical image computing and computer-assisted intervention*, pp. 234–241. Springer, 2015. (cited on p. 1)
- Scarselli, F., Gori, M., Tsoi, A. C., Hagenbuchner, M., and Monfardini, G. The graph neural network model. *IEEE transactions on neural networks*, 20(1):61–80, 2008. (cited on p. 1)
- Sen, P., Namata, G., Bilgic, M., Getoor, L., Galligher, B., and Eliassi-Rad, T. Collective classification in network data. *AI Magazine*, 29(3):93, Sep. 2008. (cited on p. 1)
- Shapson-Coe, A., Januszewski, M., Berger, D. R., Pope, A., Wu, Y., Blakely, T., Schalek, R. L., Li, P., Wang, S., Maitin-Shepard, J., Karlupia, N., Dorkenwald, S., Sjostedt, E., Leavitt, L., Lee, D., Bailey, L., Fitzmaurice, A., Kar, R., Field, B., Wu, H., Wagner-Carena, J., Aley, D., Lau, J., Lin, Z., Wei, D., Pfister, H., Peleg, A., Jain, V., and Lichtman, J. W. A connectomic study of a petascale fragment of human cerebral cortex. *bioRxiv*, 2021. doi: 10.1101/2021.05.29.446289. URL <https://www.biorxiv.org/content/early/2021/05/30/2021.05.29.446289>. (cited on p. 1)
- Srinivasa, R. S., Xiao, C., Glass, L., Romberg, J., and Sun, J. Fast graph attention networks using effective resistance based graph sparsification, 2020. (cited on p. 1)

- Sun, F.-Y., Hoffman, J., Verma, V., and Tang, J. InfoGraph: unsupervised and semi-supervised graph-level representation learning via mutual information maximization. In *International Conference on Learning Representations*, 2020. URL <https://openreview.net/forum?id=r11fF2NYvH>. (cited on p. 2)
- Topping, J., Giovanni, F. D., Chamberlain, B. P., Dong, X., and Bronstein, M. M. Understanding over-squashing and bottlenecks on graphs via curvature, 2021. (cited on p. 2)
- Vaswani, A., Shazeer, N., Parmar, N., Uszkoreit, J., Jones, L., Gomez, A. N., Kaiser, Ł., and Polosukhin, I. Attention is all you need. In Guyon, I., Luxburg, U. V., Bengio, S., Wallach, H., Fergus, R., Vishwanathan, S., and Garnett, R. (eds.), *Advances in Neural Information Processing Systems*, volume 30. Curran Associates, Inc., 2017. URL <https://proceedings.neurips.cc/paper/2017/hash/3f5ee243547dee91fbd053c1c4a845aa-Abstract.html>. (cited on p. 1)
- Wu, Z., Zeng, M., Qin, F., Wang, Y., and Kosinka, J. Active 3-d shape cosegmentation with graph convolutional networks. *IEEE computer graphics and applications*, 39(2): 77–88, 2019. (cited on p. 1)
- Xu, K., Hu, W., Leskovec, J., and Jegelka, S. How powerful are graph neural networks? In *International Conference on Learning Representations*, 2019. URL <https://openreview.net/forum?id=ryGs6iA5Km>. (cited on pp. 2 and 5)
- Yang, Z., Yu, Y., You, C., Steinhardt, J., and Ma, Y. Rethinking bias-variance trade-off for generalization of neural networks. In III, H. D. and Singh, A. (eds.), *Proceedings of the 37th International Conference on Machine Learning*, volume 119 of *Proceedings of Machine Learning Research*, pp. 10767–10777. PMLR, 13–18 Jul 2020. URL <https://proceedings.mlr.press/v119/yang20j.html>. (cited on p. 2)
- Zeng, H., Zhou, H., Srivastava, A., Kannan, R., and Prasanna, V. GraphSAINT: graph sampling based inductive learning method. In *International Conference on Learning Representations*, 2020. URL <https://openreview.net/forum?id=BJe8pkHFwS>. (cited on p. 1)

A. Proofs

A.1. Proof of Lemma 1

For each $h \in U$, define continuous function $k(h, \cdot) = \phi_h(\cdot)$, and construct the following functional space:

$$\mathcal{H}_0 = \text{span}(\{\phi_h(\cdot) \mid \forall h \in U\}) \quad (\text{A.15})$$

Define an inner product on \mathcal{H}_0 by:

$$\left\langle \sum_{i=1}^n a_i \phi_{h_i}(\cdot), \sum_{j=1}^m b_j \phi_{h_j}(\cdot) \right\rangle = \sum_{i=1}^n \sum_{j=1}^m a_i b_j k(h_i, h_j) \quad (\text{A.16})$$

Let \mathcal{H} be the completion of \mathcal{H}_0 with respect to this inner product. Now \mathcal{H} is an RKHS built from kernel $k(\cdot, \cdot)$.

Since $k(\cdot, \cdot)$ is universal (Micchelli et al., 2006), the set \mathcal{H} is dense in $C(U)$ with respect to the supremum norm, i.e., for any $f \in C(U)$:

$$\forall \epsilon > 0 \exists g \in \mathcal{H} \text{ s.t. } \sup_{h \in U} |f(h) - g(h)| < \epsilon \quad (\text{A.17})$$

In addition, \mathcal{H} has reproducing property:

$$\forall f \in \mathcal{H} \forall h \in U \quad f(h) = \langle f, \phi_h(\cdot) \rangle \quad (\text{A.18})$$

and thus we have:

$$\rho(Y|H) = \inf_{Z \in \mathcal{C}_H} d(Y, Z) = \inf_{f \in C(U)} d(Y, f(H)) = \quad (\text{A.19})$$

$$= \inf_{f \in \mathcal{H}} d(Y, f(H)) = \inf_{f \in \mathcal{H}} d(Y, \langle f, \phi_H(\cdot) \rangle) \quad (\text{A.20})$$

A.2. Proof of Lemma 2

We denote the estimation of ρ on a finite collection of samples $(h, y) = \{(h_n, y_n)\}_{n \in [N]}$ by ρ^* and use the distance induced from l_p -norm, where $p \in [1, \infty)$. Thus we have:

$$\rho^*(Y|H) = \inf_{f \in \mathcal{H}} \left(\frac{1}{N} \sum_{i \in [N]} |y_i - \langle f, \phi_{h_i}(\cdot) \rangle|^p \right)^{1/p} \quad (\text{A.21})$$

From the *representer theorem* (Kimeldorf & Wahba, 1970) there exists $f^* \in \mathcal{H}$ of the following form:

$$f^* = \sum_{i \in [N]} \alpha_i \phi_{h_i}(\cdot) \quad (\text{A.22})$$

which minimizes $\rho^*(Y|H)$. Thus:

$$\rho^*(Y|H) = \left(\frac{1}{N} \sum_{i \in [N]} |y_i - \langle f^*, \phi_{h_i}(\cdot) \rangle|^p \right)^{1/p} = \quad (\text{A.23})$$

$$= \min_{\alpha_j \in \mathbb{R}} \left(\frac{1}{N} \sum_{i \in [N]} |y_i - \sum_{j \in [N]} \alpha_j k(h_i, h_j)|^p \right)^{1/p} = \quad (\text{A.24})$$

$$= \min_{\alpha \in \mathbb{R}^N} \frac{1}{N^{1/p}} \|y - K\alpha\|_p \quad (\text{A.25})$$

where $K_{ij} = k(h_i, h_j)$ is a Gram matrix.

A.3. Proof of Theorem 1

Given:

$$\rho^*(Y|H) = \min_{\alpha \in \mathbb{R}^N} \frac{1}{N^{1/p}} \|y - K\alpha\|_p \quad (\text{A.26})$$

decompose y into two parts:

$$y = y_{\parallel} + y_{\perp} \quad (\text{A.27})$$

where $y_{\parallel} \in \text{im}(K)$ and $\forall v \in \text{im}(K) \quad y_{\perp}^T v = 0$. Then we have:

$$\rho^*(Y|H) = \frac{1}{N^{1/p}} \|y_{\perp}\|_p \quad (\text{A.28})$$

Since K is positive semi-definite, we have the following eigendecomposition:

$$K = U\Lambda U^T \quad (\text{A.29})$$

where columns of unitary matrix U are eigenvectors of K and Λ is a diagonal matrix of eigenvalues.

Let:

$$\lambda_1, \lambda_2, \dots, \lambda_k, 0, 0, \dots, 0 \quad (\text{A.30})$$

be the descending order of eigenvalues, where $\lambda_k > 0$. Then:

$$\Pi = \sum_{i \in [k]} u_i u_i^T \quad (\text{A.31})$$

is an orthogonal projection into $\text{im}(K)$ subspace. Consequently:

$$\rho^* = \frac{1}{N^{1/p}} \|(\mathbb{I} - \Pi)y\|_p \quad (\text{A.32})$$

where \mathbb{I} is an identity matrix.

B. Theoretical results

When $p = 2$ we can compute the theoretical recoverability loss in the following way:

$$\rho(Y|X) = \sqrt{\mathbb{E}[(Y - \mathbb{E}[Y|X])^2]} \quad (\text{B.33})$$

Theoretical recoverability loss for Table 1

$$\mathbb{E}[Z|X] = Z \Rightarrow \rho(Z|X) = \sqrt{\mathbb{E}[(Z - Z)^2]} = 0 \quad (\text{B.34})$$

$$\mathbb{E}[X|Z] = X \Rightarrow \rho(X|Z) = \sqrt{\mathbb{E}[(X - X)^2]} = 0 \quad (\text{B.35})$$

$$\mathbb{E}[W|X] = W \Rightarrow \rho(W|X) = \sqrt{\mathbb{E}[(W - W)^2]} = 0 \quad (\text{B.36})$$

$$\mathbb{E}[X|W = w] = \quad (\text{B.37})$$

$$= \mathbb{E}[\mathbb{1}_{X \geq 0} X | W = w] + \mathbb{E}[\mathbb{1}_{X < 0} X | W = w] = \quad (\text{B.38})$$

$$= \mathbb{E}[\mathbb{1}_{\sqrt{w} \geq 0} \sqrt{w}] + \mathbb{E}[\mathbb{1}_{-\sqrt{w} < 0} (-\sqrt{w})] = 0 \quad (\text{B.39})$$

$$\rho(X|W) = \sqrt{\mathbb{E}[(X - 0)^2]} = 1 \quad (\text{B.40})$$

Theoretical recoverability loss for Fig. 3

$$\mathbb{E}[Y|X = x] = \sum_{i \in [100]} (x_i + \alpha \cdot N_i) = \sum_{i \in [100]} x_i \quad (\text{B.41})$$

$$\mathbb{E}[Y|X] = \sum_{i \in [100]} X_i \quad (\text{B.42})$$

$$\rho(Y|X) = \sqrt{\mathbb{E}[(Y - \sum_{i \in [100]} X_i)^2]} = |\alpha| \sqrt{100} \quad (\text{B.43})$$

C. Embedding types used in experiments on real data

- GraphConv:

$$x'_i = \Theta_1 x_i + \Theta_2 \sum_{j \in N(i)} e_{ji} x_j \quad (\text{C.44})$$

where Θ_1 and Θ_2 are trainable parameters.

- GCNConv:

$$x'_i = \Theta \sum_{j \in N(i) \cup \{i\}} \frac{e_{ji}}{\sqrt{\hat{d}_j \hat{d}_i}} x_j \quad (\text{C.45})$$

where $\hat{d}_i = 1 + \sum_{j \in N(i)} e_{ji}$, and Θ are trainable parameters.

- SAGEConv:

$$x'_i = W_1 x_i + W_2 \text{mean}_{j \in N(i)} \{x_j\} \quad (\text{C.46})$$

where W_1 and W_2 are trainable parameters.

- GINConv:

$$x'_i = h_{\Theta} \left((1 + \epsilon) x_i + \sum_{j \in N(i)} x_j \right) \quad (\text{C.47})$$

where h_{Θ} is an MLP and ϵ could be trainable.

- GATv2Conv:

$$x'_i = \alpha_{ii} \Theta x_i + \sum_{j \in N(i)} \alpha_{ij} \Theta x_j \quad (\text{C.48})$$

where:

$$\alpha_{ij} = \frac{\exp(a^T \text{LeakyReLU}(\Theta[x_i || x_j]))}{\sum_{k \in N(i) \cup \{i\}} \exp(a^T \text{LeakyReLU}(\Theta[x_i || x_k]))} \quad (\text{C.49})$$

and Θ are trainable parameters.

C.1. Technical notes

- There is a numerical instability in gradient computation of eigendecomposition $K = U\Lambda U^T$. The problem comes from equal eigenvalues in:

$$\frac{\partial L}{\partial K} = U \left\{ \left(\tilde{K}^T \circ \left(U^T \frac{\partial L}{\partial U} \right) \right) + \left(\frac{\partial L}{\partial \Lambda} \right)_{diag} \right\} U^T \quad (\text{C.50})$$

where:

$$\tilde{K}_{ij} = \begin{cases} \frac{1}{\lambda_i - \lambda_j}, & i \neq j \\ 0, & i = j \end{cases} \quad (\text{C.51})$$

and $(\cdot)_{diag}$ means all off-diagonal elements set to 0. To overcome this issue, we changed \tilde{K} to be:

$$\tilde{K}_{ij} = \begin{cases} \frac{1}{\lambda_i - \lambda_j}, & \lambda_i \neq \lambda_j \\ \frac{1}{\epsilon}, & \lambda_i = \lambda_j \\ 0, & i = j \end{cases} \quad (\text{C.52})$$

- When we perform eigendecomposition, we do not have explicit zero eigenvalues. Thus instead of taking the first k non-zero eigenvalues, we simply clamp them between 0 and 1.